

Welcome

New Mexico Chapter
of
AVS – The Science & Technology Society

53rd Symposium

Technical Sessions
Poster Competition

May 16, 2017

Sheraton Albuquerque Airport Hotel
Albuquerque, New Mexico

Short Courses

May 15-18, 2017

David Adams, Chair

dadams205@comcast.net

Vendor Show

May 16, 2017

Guild Copeland, Chair

gcopeavs@comcast.net



*Science and Technology
of Materials, Interfaces and Processing*

Table of Contents



Welcome	3
New Mexico Chapter Officers and Committees	4
New Mexico Chapter Background	5
Sheraton Floor Plan & Symposium Events	6
Vendor Exhibit	7
Technical Session Program	8
Abstracts	11

Welcome to the 53rd NMAVS Symposium!

Welcome to the 2017 NMAVS Chapter Symposium. This year's Symposium is embedded in a busy week for the NMAVS Chapter with short courses, business luncheon, and vendor show. The Symposium exhibits talks and posters from multiple materials science perspectives as demonstrated by the diverse range of topics on the schedule. We are fortunate to have participation from professors, staff scientists, post-docs, and students throughout the region.

The New Mexico Chapter of AVS draws membership from New Mexico, Arizona, Oklahoma, and the portion of Texas in the Mountain Time Zone. The Chapter is now over 50 years old and has committed, long-lasting participation from its members. Growth of the Chapter is continuing as we develop plans for starting a student chapter from Universities within the region. We make significant efforts to contribute to the community through science fair support, scholarships, high-school teacher support, and other local events. The New Mexico Chapter of AVS also established the Thin Film Division Distinguished Technologist Award at AVS to reward the accomplishments of technical support staff.

The annual New Mexico AVS Symposium highlights our scientific contributions related to Science and Technology of Materials, Interfaces, and Processing. The accompanying short courses play a vital role in training new scientists in the field and in supporting the Chapter.

We thank you for your involvement and look forward to your continued participation in AVS and in the New Mexico Chapter of AVS.

Erica Douglas & Michael Brumbach
2017 Symposium Chairs

THE NEW MEXICO CHAPTER OF THE AVS – THE SCIENCE AND TECHNOLOGY SOCIETY

<i>Chair:</i>	Kateryna Artyushkova	<i>University of New Mexico</i>
<i>Vice Chair:</i>	Michael Brumbach	<i>Sandia National Laboratories</i>
<i>Treasurer:</i>	Todd Bauer	<i>Sandia National Laboratories</i>
<i>Secretary:</i>	Randy Shul	<i>Sandia National Laboratories</i>
<i>Past Chair:</i>	Erica Douglas	<i>Sandia National Laboratories</i>

Executive Committee

Anthony Muscat	<i>University of Arizona</i>
Darin Leonhardt	<i>Sandia National Laboratories</i>
Stefan Zollner	<i>New Mexico State University</i>
Nicholas Argibay	<i>Sandia National Laboratories</i>
James A. (Tony) Ohlhausen	<i>Sandia National Laboratories</i>
David Henry	<i>Sandia National Laboratories</i>

AVS/NM Committee Chairs

EDUCATION	V. Carter Hodges	<i>Sandia National Laboratories</i>
HISTORIAN	Woody Weed	<i>Sandia National Laboratories</i>
SCHOLARSHIPS & STUDENT AWARDS	Craig Nakakura	<i>Sandia National Laboratories</i>
SCIENCE FAIR COORDINATOR	Kateryna Artyushkova	<i>University of New Mexico</i>

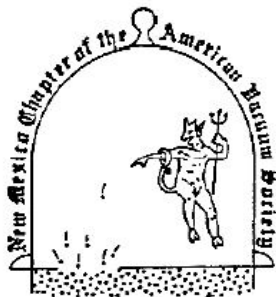
Symposium Organizing Committee

CHAIR	Erica Douglas	<i>Sandia National Laboratories</i>
CHAIR	Michael Brumbach	<i>Sandia National Laboratories</i>
VENDOR SHOW CHAIR	Guild Copeland	<i>Sandia National Laboratories</i>
SHORT COURSE CHAIR	David P. Adams	<i>Sandia National Laboratories</i>
LOCAL ARRANGEMENTS	Amy P. Bauer	
WEBMASTER	James (Tony) Ohlhausen	<i>Sandia National Laboratories</i>

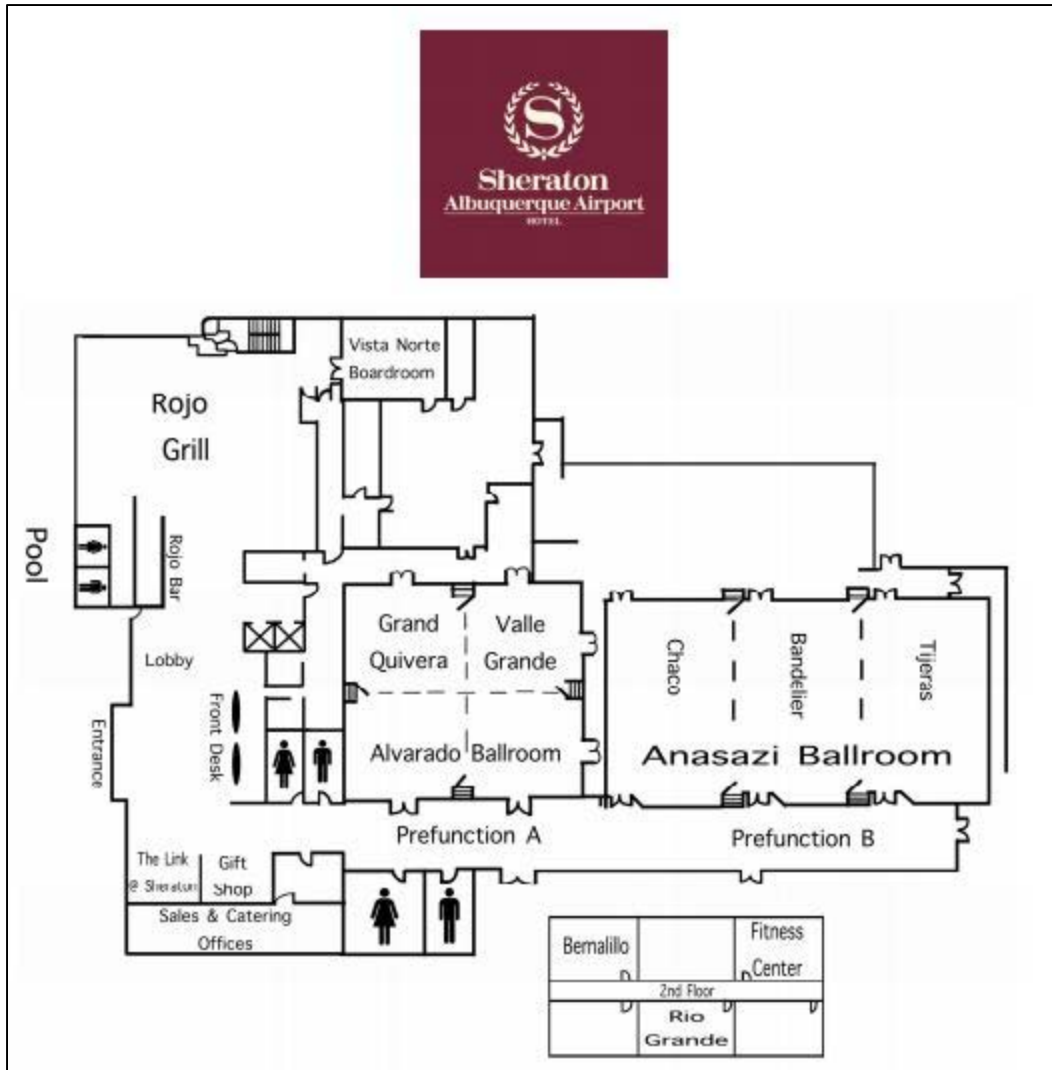
New Mexico Chapter

AVS – The Science and Technology Society

The logo of the New Mexico Chapter of AVS illustrates a scientific caricature known as Maxwell's Demon, in the process of ejecting gas molecules from a bell Jar. One of James Clark Maxwell's accomplishments was the formulation of a statistical theory of gas behavior. One conclusion of this theory is that it is statistically possible, although highly improbable, for all gas molecules in a container to spontaneously move to one corner, thereby creating a vacuum in the rest of the container. Since the concept that random motion of gas molecules could create a vacuum was unacceptable to many, the humorous alternative of a small invisible demon who herded the molecules toward the corner, or an exit, was invented. A variation on this theme appears in the NM Chapter AVS information above, where the Zia Sun symbol (the New Mexico State Symbol) has replaced the bell jar, and Maxwell's Demon is represented in the form of a Zuni flute player.



Maxwell's Demon



VENDOR SHOW ACTIVITIES

Buffet Luncheon

Tuesday, May 16

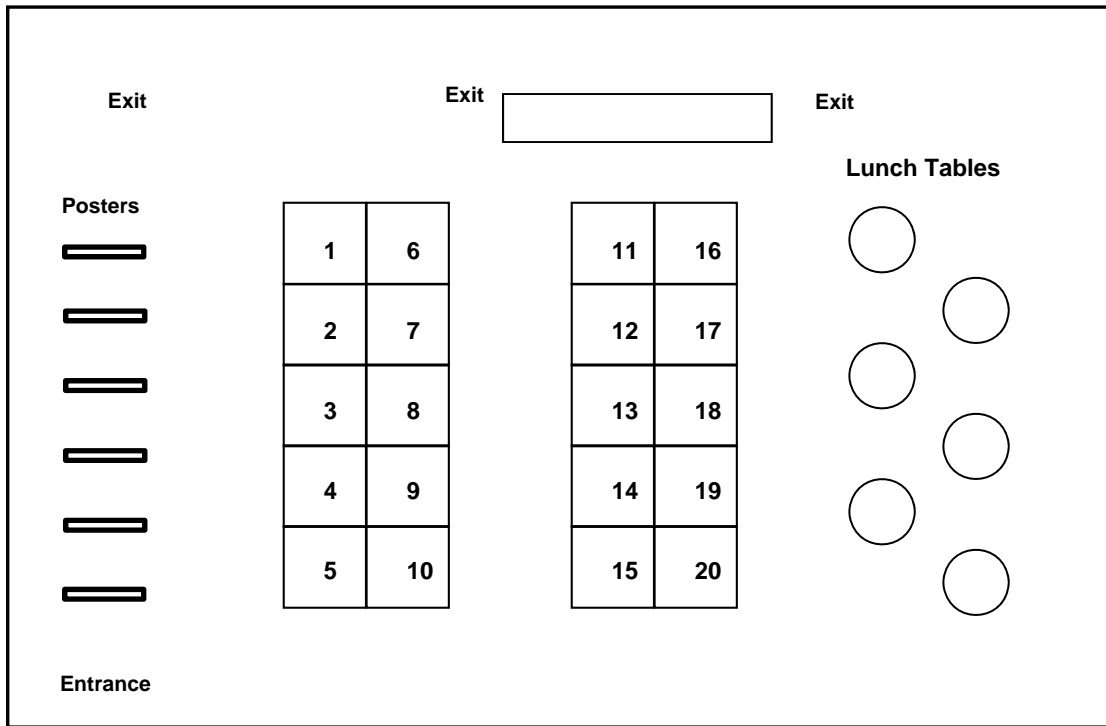
A buffet luncheon will be available in the vendor exhibit hall (Anasazi Ballroom) at 11:30am for all Symposium, Short Course and Equipment Exhibit Attendees.

Door Prizes in Vendor Show

Tuesday, May 16

Participants in the vendor show may register for a drawing to win a door prize. Forms for the drawings will be available at the entrance to the exhibit hall. The vendor show and all associated activities are open to the public at no charge. Members of the NMAVS Executive Committee, the Symposium Organizing Committee, and registration booth workers are not eligible for door prizes.

Vendor Exhibit Booth Locations • Anasazi Ballroom



- | | |
|--------------------------------|--------------------------------------|
| 1 InstruTech | 11 Williams Associates |
| 2 Telesis HV, LLC | 12 Agilent Technologies, Inc. |
| 3 Swagelok Southwest | 13 Physical Electronics |
| 4 Trillium US | 14 Scientific Vacuum Sales & Support |
| 5 Pfeiffer Vacuum | 15 MDC Vacuum Products, LLC |
| 6 J.F. Hurlbut Co. | 16 Kurt J. Lesker Company |
| 7 Ideal Vacuum Products LLC | 17 Leybold USA, Inc. |
| 8 GNB Corporation | 18 Edwards Vacuum |
| 9 ULVAC Technologies, Inc | 19 JB Technical, LLC |
| 10 Synergy Systems Corporation | 20 Nor-Cal Products |

NMAVS Symposium Schedule of Events

Gran Quivera I Meeting Room

TUESDAY, MAY 16, 2017

7:45 **UPLOAD OF MORNING PRESENTATIONS**

8:00 **ERICA DOUGLAS / MICHAEL BRUMBACH**, Welcome

SESSION 1: THIN FILM SCIENCE, MODERATOR: ERICA DOUGLAS

8:05 **PABITRA CHOUDHURY**, New Mexico Institute of Mining and Technology, *Engineering of 2-D Surfaces: Applications in Electronics and Energy*

8:25 **SEAN SMITH**, Sandia National Laboratories, *Pyroelectric Response in $Hf_{1-x}Zr_xO_2$ Thin Films*

8:45 **ISAAC RUIZ**, Sandia National Laboratories, *Finding Graphene: Observing Atomically Thin Materials Encapsulated in Dielectrics*

9:05 **MOHAMMAD ABDULLAH-AL-MAMUN**, New Mexico State University, *Effects of Nb Doping on Structural and Electrical Properties on PZT Thin Films*

9:25 **NUWANJULA SAMARASINGHA**, New Mexico State University, *Excitonic Effect at Interfaces in Thin Oxide Films*

9:45 **BREAK – REFRESHMENTS IN ANASAZI BALLROOM**

SESSION 2: ELECTROCHEMISTRY, MODERATOR: MICHAEL BRUMBACH

10:00 **INVITED SPEAKER: SVITLANA PYLYPENKO**, Colorado School of Mines, *Characterization of Electrocatalytic Materials: Challenges and Novel Approaches*

10:40 **TYLAN WATKINS**, Sandia National Laboratories, *Predicting Lithium Polysulfide Solubility and Reaction Pathway Using a Unique Donicity Scale for Li-S Electrolytes*

11:00 **SADIA KABIR**, University of New Mexico, *Developing Nitrogen Doped 3D-Graphene Nanosheets as Activated Supports for Oxygen Electroreduction in Fuel Cells*

11:20 **HANQING PAN**, New Mexico Institute of Mining and Technology, *Efficient Photoreduction of Bicarbonate to Formate Catalyzed by Gold-TiO₂ Composite Nanocatalyst under Solar Light*

11:40 **LUNCH IN ANASAZI BALLROOM**

VENDOR SHOW IN ANASAZI BALLROOM

POSTER SESSION IN ANASAZI BALLROOM

1. **NABIL SHAIKH**, University of New Mexico, *Comparison of Reaction of Synthesized and Commercial Manganese Oxide with Bisphenol A*
2. **SADIA KABIR**, University of New Mexico, *Investigating the Performance of Pd/3DGraphene Nanocomposites in Anion Exchange Membrane Fuel Cells*
3. **JOSEPH KERWIN**, New Mexico Institute of Mining and Technology, *Gelatin Characterization for Tissue Biomimetic for studying the Mechanisms Blast Induced Traumatic Brain Injuries*
4. **KEENIYA-GAMALAGE-GEHAN DE SILVA**, New Mexico Institute of Mining and Technology, *Direct Photocatalytic Reduction of Bicarbonate to Formate on Plasmonic Metallic Nanoparticles*
5. **MICHAEL MARQUEZ**, Sandia National Laboratories, *Physical Vapor Deposition of Explosive Materials*
6. **MD MOSADDEK HOSSEN**, University of New Mexico, *Three Dimensional Structural Analysis of Electrodes for Fuel Cells and Electrolyzers Using FIB-SEM*
7. **MORGAN O'MAHONY**, Sandia National Laboratories, *Precision Backside Si Thinning to Land on Thin Films*
8. **THALIA QUINN**, New Mexico Institute of Mining and Technology, *C-H Bond Activation on Single-Site Active Porous Sheet: Catalytic Conversion of Methane to Methanol*
9. **CHARLES GRIEGO**, New Mexico Institute of Mining and Technology, *Theoretical Study of a High Performance Thermoelectric Material: Stanene*
10. **MICHAEL SALCIDO**, Sandia National Laboratories, *Optimizing a Plasma Process for Creating Black Silicon*
11. **ERIN SOVEY**, Sandia National Laboratories, *Creating Facets in Photoresist Using Plasma Etch Processing*
12. **CARMEN A. VELASCO**, University of New Mexico, *Study of Effects of Organic Matter and Uranium Binding (Release) from Abandoned Mine Lands in the Southwestern United States*

SESSION 3: OPTICS AND SPECTROSCOPY, MODERATOR: ERICA DOUGLAS

- 1:15 **UPLOAD OF AFTERNOON PRESENTATIONS**
- 1:30 **STEPHEN HOWELL**, Sandia National Laboratories, *Graphene-Based Charge-Coupled Devices for Sensitive Optical Detection*
- 1:50 **CAROLA EMMINGER**, New Mexico State University, *Temperature Dependence of the Dielectric Function of Bulk Ge*
- 2:10 **JACQUELINE COOKE**, New Mexico State University, *Near-Infrared to Vacuum Ultraviolet (VUV) Dielectric Properties of LaAlO₃*
- 2:30 **NABIL SHAIKH**, University of New Mexico, *Spectroscopic Surface Study of Manganese Oxides Reaction with Organic Micropollutants*
- 2:50 **BREAK – REFRESHMENTS IN ANASAZI BALLROOM**

SESSION 4: MATERIALS SCIENCE AND CHARACTERIZATION, MODERATOR: LINNEA ISTA

- 3:00 **MICHAEL LEE**, Northern Arizona University, *Design of a Time-of-Flight Secondary Ion Mass Spectrometer for Hands-on Undergraduate Instruction*
- 3:20 **FARZIN ABADIZAMAN**, New Mexico State University, *Temperature Dependent Mueller Matrix Measurements of Magnetised Ni near the Curie Temperature*
- 3:40 **SARUN ATIGANYANUN**, University of New Mexico, *Microsphere-Based Disordered Coatings for Effective Radiative Cooling*
- 4:00 **YECHUAN CHEN**, University of New Mexico, *Fe-N-C PGM-free ORR Catalysts Derived by C-N-C Backbone Polymerization-Pyrolysis Method*
- 4:20 **DISCUSSION FOR AVS STUDENT CHAPTER (AND BREAK FOR JURY DECISIONS)**
- 4:50 **ANNOUNCEMENT OF AWARDS**
- 5:00 **ADJOURN**



Abstracts



Session 1

**Tuesday, May 16
8:05am-10:00am**

Moderator: Erica Douglas

8:05 am

Engineering of 2-D Surfaces: Applications in Electronics and Energy

Pabitra Choudhury¹

¹New Mexico Institute of Mining and Technology

Engineering of 2-D Surfaces: Applications in Electronics and Energy
2-D materials are single or tri-layer networks of atoms, such as carbon, hBN, and MoS₂. The 2D materials provide ballistic transport of charge carriers as well as carrier confinement, which are essentially attractive features for low power future electronic devices. These devices require deposition of thin uniform dielectrics between two semiconducting layers. However 2D semiconductors such as graphene, boron nitride, and some metal dichalcogenides (MDCs) are un-reactive, thus the dielectric layer selectively nucleates on defect sites or step edges rather than all over the surface uniformly. It is however possible to overcome this difficulty via ALD process. We have used combined density functional theory (DFT) calculations and experimental approach to develop this material. Another important application of 2-D surfaces is in Energy. We will discuss Three different applications: (i) oxygen reduction reaction (ORR) occurring at the cathode side of any fuel cells, (ii) catalytic conversion of natural gas to liquid feed stock at mild reaction conditions, and (iii) Anhydrous proton transport membrane for hydrogen fuel cells.



8:25 am

Pyroelectric Response in $\text{Hf}_{1-x}\text{Zr}_x\text{O}_2$ Thin Films

Sean Smith¹, Andrew Kitahara¹, David Henry¹, Michael Brumbach¹,
Mark Rodriguez¹, Jon Ihlefeld¹

¹Sandia National Laboratories

Switchable polarization in HfO_2 -based thin films was first reported in 2011 and has since been shown with a variety of dopants. Process compatibility with current silicon microelectronics make it an appealing alternative to traditional ferroelectrics. A growing body of literature supports ferroelectric response, including, recently, pyroelectricity. Pyroelectric reports to date utilized measurements that may contain artifacts, which mask the response. We explore the pyroelectric response in 20 nm thick atomic layer deposited (ALD) $\text{Hf}_{1-x}\text{Zr}_x\text{O}_2$ films using a cyclic heating and cooling technique that allows decoupling of pyroelectric response from thermally stimulated currents. This work will explore the influence of composition on pyroelectric performance in $\text{Hf}_{0.5}\text{Zr}_{0.5}\text{O}_2$.

Sandia National Laboratories is a multiprogram laboratory operated by Sandia Corporation, a wholly owned subsidiary of Lockheed Martin Company, for the United States Department of Energy's National Nuclear Security Administration under contract DE-AC04-94AL85000.



8:45 am

Finding Graphene: Observing Atomically Thin Materials Encapsulated in Dielectrics

Isaac Ruiz¹, Michael D. Goldflam¹, Thomas E. Beechem¹,
Bruce L. Draper¹, Stephen W. Howell¹, Anthony E. McDonald¹

¹Sandia National Laboratories

In this work, the authors revisit the topic of optical visibility of graphene on dielectric substrates and extend it to dielectrically encapsulated graphene films. Although previously flirted with through simulations, here for the first time, the optical contrast of SiO₂ encapsulated graphene films were measured experimentally for varying dielectric thicknesses in the visible wavelengths and a consistent model was developed. The model was then used to predict the contrast of graphene films encapsulated in HfO₂, Al₂O₃, and Si₃N₄, which are other common dielectrics used in graphene device fabrication. Thus, tuning of the graphene's visibility may now be predicted through careful consideration of the dielectric and top and/or bottom dielectric thicknesses. Furthermore, the contrast calculations may also serve as method to determine residual contamination and general film metrology. Because encapsulation is needed to passivate the graphene in order to stabilize the films electrical properties, this work lends itself towards practical graphene device and component fabrication, as well as characterization. Most importantly, because the results presented were done so with commercially available graphene and standard fabrication processes, ensuring wide applicability of the results in the present and in the future, as maturation of graphene processing occurs.

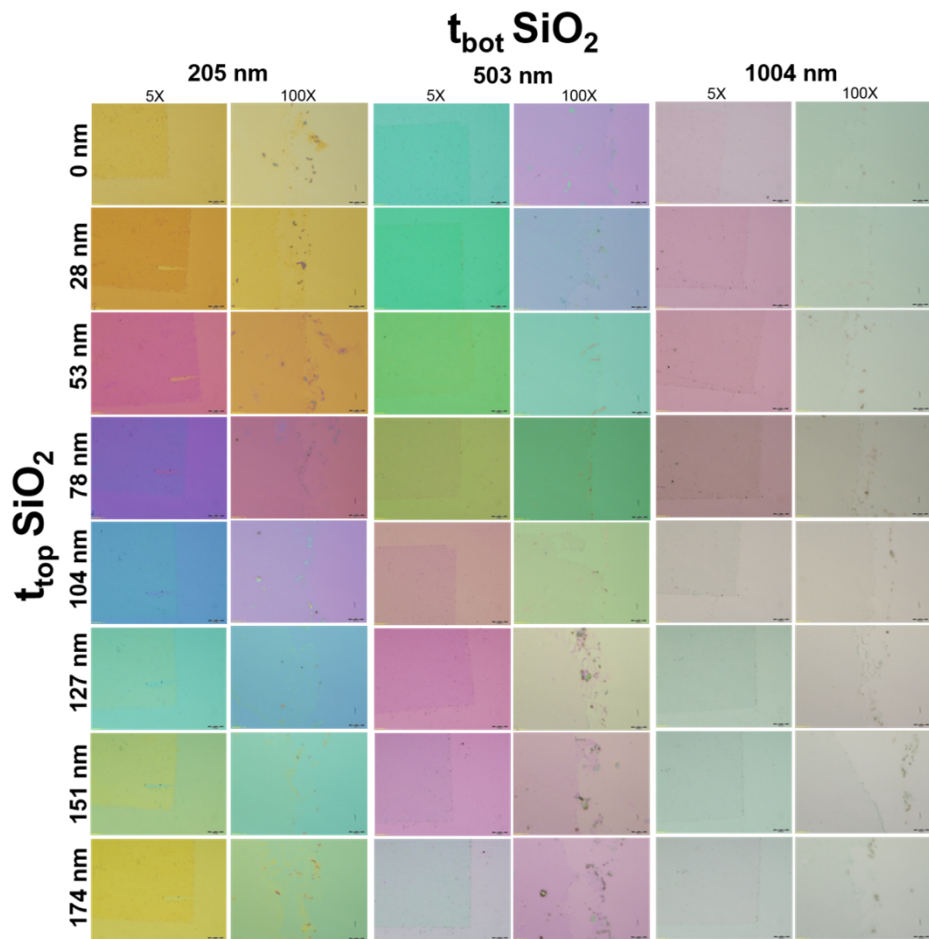


8:45 am
continued

Finding Graphene: Observing Atomically Thin Materials Encapsulated in Dielectrics

Isaac Ruiz¹, Michael D. Goldflam¹, Thomas E. Beechem¹,
Bruce L. Draper¹, Stephen W. Howell¹, Anthony E. McDonald¹

¹Sandia National Laboratories



9:05 am

Effects of Nb Doping on Structural and Electrical Properties on PZT Thin Films

Mohammad Abdullah-Al-Mamun¹, Dmitry Karpov¹,
Edwin Fohtung^{1,2}

¹New Mexico State University, ²Los Alamos National Laboratory

Lead Zirconate titanate PZT ($\text{Pb}[\text{Zr}_x\text{Ti}_{1-x}]\text{O}_3$) is a piezoelectric materials widely used in memory applications, sensors and actuators. In such device application, a major challenge is how to accurately estimate structural properties to improve on functionality. The structural properties such as lattice strain, ferroelectric displacements and piezoelectric coefficient of PZT and Nb doped PZT, PNZT ($\text{Pb}[\text{Nb}_y(\text{Zr}_{1-x}\text{Ti}_x)_{1-y}]\text{O}_3$) was studied using high resolution x-ray diffraction and Bragg coherent diffraction. Under an external electric field a PZT and PNZT thin film showed significantly different P-E ferroelectric hysteresis. We attribute these changes to the role of Nb defects in PZT and its effects on the nature of the ferroelectric domains and domain wall.



9:25 am

Excitonic Effect at Interfaces in Thin Oxide Films

Nuwanjula Samarasingha¹, Cesar Rodriguez¹, Jaime Moya¹,
Nalin Fernando¹, Stefan Zollner¹, Patrick Ponath²,
Kristy J. Kormondy², Alex Demkov², Dipayan Pal³, Aakash Mathur³,
Ajaib Singh³, Surjendu Dutta³, Jaya Singhal³,
Sudeshna Chattopadhyay³

¹New Mexico State University, ²University of Texas at Austin,
³Indian Institute of Technology Indore

The presence of excitonic features in the optical constants and ellipsometry spectra of bulk semiconductors and insulators has been known for many years. In Si, Ge, and GaAs, the E_1 critical points are strongly enhanced by two-dimensional excitons. Three-dimensional excitons have been seen in ellipsometry spectra for GaP and Ge. Excitons also influence the dielectric function (ϵ) of SrTiO₃. The influence of excitonic absorption on the ϵ was described by Tanguy.

In a thin epitaxial layer on a substrate with a different band gap, the wave functions of the electron and hole are strongly modified. In a thin type-I quantum well, both the electron and the hole are confined, which leads to an increase in the dipole overlap matrix element. Therefore, the dominant absorption peak at 4.2 eV is larger in a 20 nm thick SrTiO₃ layer on a LaAlO₃ substrate than in bulk SrTiO₃.

On the other hand, in a staggered type-II quantum well the overlap dipole matrix element is strongly reduced. If a SrTiO₃ layer is grown on Si or Ge, the valence band maximum occurs in the substrate, while the conduction band offset is very small. Therefore, the exciton wave function is delocalized, which reduces the dipole overlap matrix element. Therefore, ϵ of thin SrTiO₃ layers on Si or Ge are much smaller than in the bulk and decrease monotonically with decreasing thickness. A similar effect can be seen for thin ZnO layers on Si as a function of thickness.

The dielectric function of SrTiO₃ is not only affected by layer thickness. A very thick polycrystalline SrTiO₃ layer on Si has a much lower ϵ than a single-crystalline SrTiO₃ substrate. In this case, we speculate that the magnitude of the ϵ is related to other Tanguy parameters, perhaps the excitonic binding energy or the exciton broadening.



9:25 am
Continued

Excitonic Effect at Interfaces in Thin Oxide Films

Nuwanjula Samarasingha¹, Cesar Rodriguez¹, Jaime Moya¹,
Nalin Fernando¹, Stefan Zollner¹, Patrick Ponath²,
Kristy J. Kormondy², Alex Demkov², Dipayan Pal³, Aakash Mathur³,
Ajaib Singh³, Surjendu Dutta³, Jaya Singhal³,
Sudeshna Chattopadhyay³

¹New Mexico State University, ²University of Texas at Austin,
³Indian Institute of Technology Indore

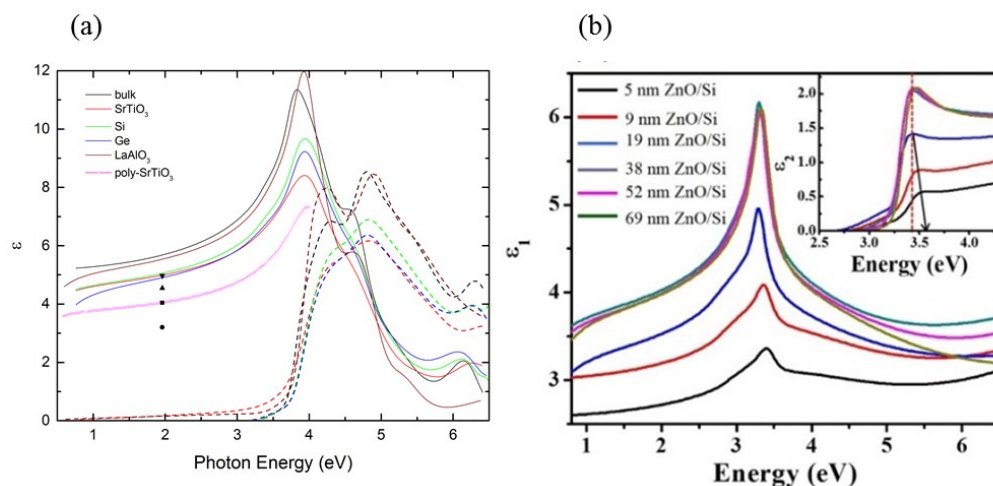


Fig: (a) Comparison of the dielectric function of SrTiO₃ films on various substrates compared to that of bulk SrTiO₃ (b) Real (ϵ_1) and imaginary part (ϵ_2) of dielectric function vs film thickness of ZnO films on Si substrates





Session 2

**Tuesday, May 16
10:00am-11:40am**

Moderator: Michael Brumbach

**Invited
10:00 am**

Characterization of Electrocatalytic Materials: Challenges and Novel Approaches

Svitlana Pylypenko¹

¹Colorado School of Mines

Advancing our understanding of electrocatalytic materials is crucial for designing next-generation electrocatalysts and devices. Activity and durability depend heavily on surface properties, which continuously evolve during different steps of electrocatalyst synthesis, electrode preparation, and fuel cell operation. This talk will discuss challenges with characterizing several classes of electrocatalysts for oxygen reduction reaction (ORR) in polymer electrolyte membrane fuel cells (PEMFCs), highlighting the necessity for multitechnique characterization at multiple length scales.

Improvements in the performance of earth-abundant, non-precious metal catalysts (NPMCs) have been made. However, the connection between chemical/morphological properties and electrochemical performance are still not well understood due to material heterogeneity and lack of atomic-level information on active site distributions. Nanoscale and atomic-level characterization of these materials will be discussed, demonstrating how elemental composition and chemical speciation information from X-ray photoelectron spectroscopy (XPS) can be complemented by nanoscale characterization using transmission electron microscopy (TEM) and energy dispersive x-ray spectroscopy (EDS) mapping, and atomic analysis using atom probe tomography (APT).

Efficient incorporation of electrocatalysts into electrodes requires information from length scales ranging from nano to micro, preferably with 3D visualization of electrode structure. Factors effecting electrode performances include catalyst content, amount of ionomer, amount and type of carbon additive, 3D nanowire morphology, and contact between the nanowires themselves and other constituents of the membrane electrode assembly (MEA). In the specific case of Ni-Pt nanowires, the prevention of Ni leaching is also imperative as Ni will poison the fuel cell, inevitably causing a significant drop in performance. Spectroscopy and microscopy results are combined with synchrotron techniques (extended x-ray absorption fine structure (EXAFS), x-ray absorption near edge structure (XANES), and transmission x-ray microscopy (TXM), demonstrating 2D and 3D visualization of composition and structure from atomic to micron scales.



10:40 am

Predicting Lithium Polysulfide Solubility and Reaction Pathway using a Unique Donicity Scale for Li-S Electrolytes

Tylan Watkins¹, Kevin Zavadil¹

¹Sandia National Laboratories

Use of electrolytes with low lithium polysulfide (Li_2S_n) solubility limits has attracted considerable interest in recent literature.¹ This strategy has been adopted by some as a means for significantly reducing polysulfide redox shuttling. Interestingly, some electrolyte compositions have not only shown promising cycling performance, but have also shown a unique discharge voltage profile lacking the typically observed two plateau response produced by sequential soluble long chain Li_2S_n to short chain Li_2S_n . This unique profile is thought to be the result of significantly suppressed concentrations of longer chain Li_2S_n .

What remains to be elucidated is a more quantitative assessment for solubility regimes in which alternative sulfur reduction pathways occur. A deeper understanding of the electrolyte characteristics dictating Li_2S_n solubility is lacking. Here, a unique ²³Na NMR-derived donor number (DN) scale is presented. Evaluation of donicity in this manner allows for direct comparisons between electrolytes utilizing different solvating species; see Figure 1a for THF and acetonitrile (AcN)-based electrolytes. It will be demonstrated that ²³Na-DN assignments are predictive of Li_2S_n solubility (Figure 1b). Finally, it will be shown that solubility can be used to predict thermodynamic redox potentials for Li-S cells as a function of discharge capacity. Figure 1c shows representative galvanostatic intermittent titration technique (GITT) experiments, performed on two different $\text{AcN}_x\text{-LiTFSI}$ electrolytes, with drastically different Li_2S_n solubility limits; the black traces follow the open circuit potentials at given capacities. Clearly, $\text{AcN}_{6,0}\text{LiTFSI}$ shows a second plateau (later discharge) at a lower potential than the early discharge plateau consistent with higher Li_2S_n solubility. Alternatively, $\text{AcN}_{2,0}\text{LiTFSI}$ shows a mid-discharge plateau higher than at early discharge consistent with a mechanism driven by a lack of solution phase species. Further details describing how these voltage profiles change as a function Li_2S_n solubility will be provided.



¹References: Cheng et al. ACS Energy Lett. 2016, 1, 503

10:40 am
Continued

Predicting Lithium Polysulfide Solubility and Reaction Pathway using a Unique Donicity Scale for Li-S Electrolytes

Tylan Watkins¹, Kevin Zavadil¹

¹Sandia National Laboratories

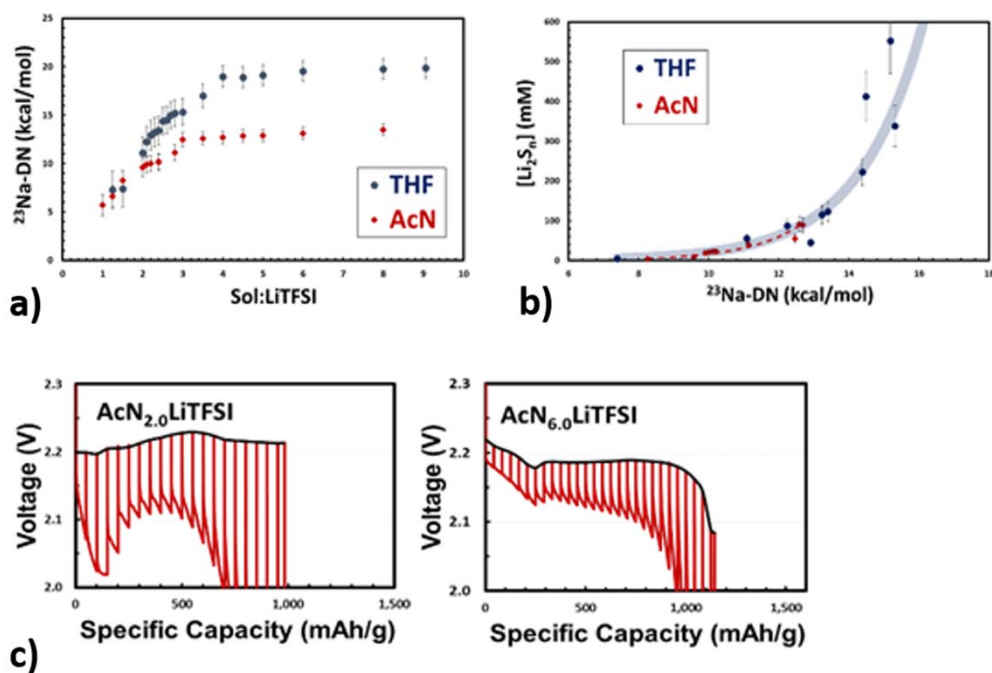


Figure 1:

- ^{23}Na NMR derived donor numbers for THF and AcN-based electrolytes, as a function of solvent to salt (LiTFSI) ratio.
- Total Concentration of lithium polysulfides with respect to the ^{23}Na -derived donor numbers for THF and AcN-based electrolytes.
- GITT measurements for $\text{AcN}_{2.0}\text{LiTFSI}$ (left) and $\text{AcN}_{6.0}\text{LiTFSI}$ (right).



11:00 am

Developing Nitrogen Doped 3D-Graphene Nanosheets as Activated Supports for Oxygen Electroreduction in Fuel Cells

Sadia Kabir¹, Kateryna Artyushkova¹, Alexey Serov¹,
Plamen Atanassov¹

¹University of New Mexico

Fuel cells are considered to be one of the most promising sustainable energy technologies for energy conversion and electric power generation. At present, graphitized materials are considered to be promising support materials for fuel cell applications. Moreover, nitrogen functionalized materials have been widely investigated for enhancing oxygen electroreduction kinetics in the cathode compartment of fuel cells.

However, the role played by nitrogen moieties towards ORR is still not clearly understood. Therefore, it is crucial to elucidate the function of nitrogen moieties while designing nitrogen-functionalized graphene or other carbon composites for the targeted incorporation of beneficial nitrogen moieties that can facilitate oxygen reduction reaction (ORR) kinetics.

In this work, porous nitrogen doped three-dimensional Graphene nanosheets (N/3D-GNS) were developed using a highly effective and previously established Sacrificial Support Method (SSM). [1-2] The synthetic parameters were varied for obtaining three major nitrogen moieties: graphitic-, hydrogenated- and pyridinic-N defect-specific nitrogen moieties. Their electrochemical properties were studied using a combination of potentiodynamic as well as spectroscopic techniques for establishing the role played by nitrogen moieties present in the 3D-GNS supports in modifying oxygen electroreduction pathways in both acidic and alkaline electrolytes.



References:

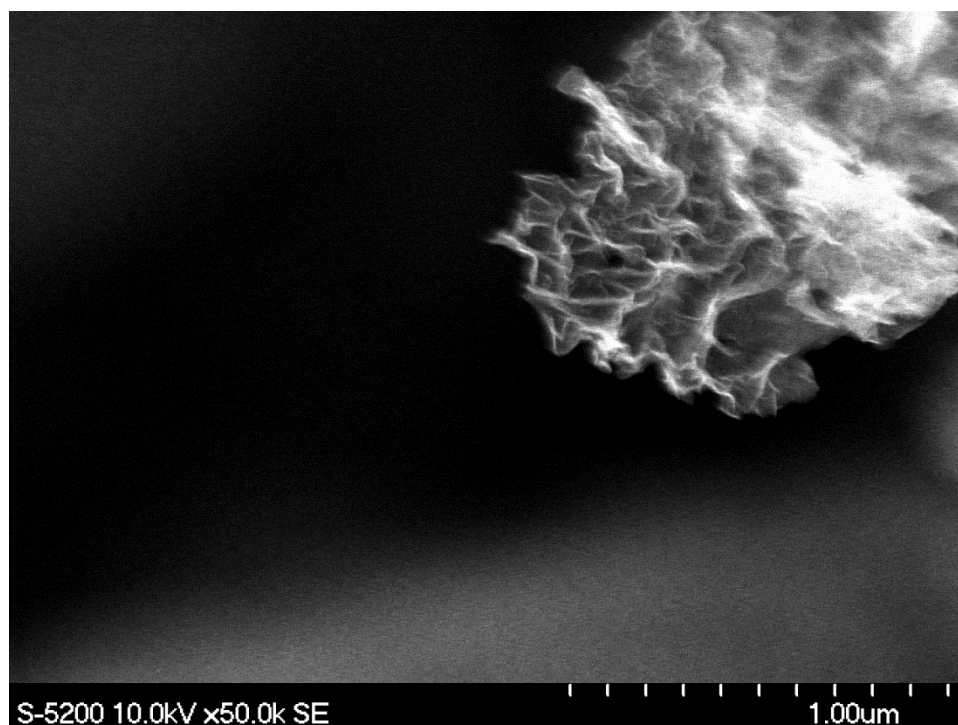
- [1] S. Kabir, A. Serov, A. Zadick, K. Artyushkova, P. Atanassov, *ChemElectroChem*, 2016; 3 (10):1655-1666.
- [2] S. Kabir, A. Serov, K. Artyushkova, P. Atanassov, *Electrochimica Acta*, 2016; 203:144-153.

**11:00 am
Continued**

Developing Nitrogen Doped 3D-Graphene Nanosheets as Activated Supports for Oxygen Electroreduction in Fuel Cells

Sadia Kabir¹, Kateryna Artyushkova¹, Alexey Serov¹,
Plamen Atanassov¹

¹University of New Mexico



Scanning Electron Microscopy image of the nitrogen doped three-dimensional graphene nanosheets (N/3D-GNS).

11:20 am

Efficient Photoreduction of Bicarbonate to Formate Catalyzed by Gold-TiO₂ Composite Nanocatalyst under Solar Light

Hanqing Pan¹, Alexzander Steiniger¹, Michael Heagy¹,
Sanchari Chowdhury¹

¹New Mexico Institute of Mining and Technology

TiO₂-catalyzed photoreduction of bicarbonate to value-added formate is studied in the presence of plasmonic gold nanoparticles. The effect of two positive hole scavengers, petroleum derived 2-propanol and green organic solvent glycerol, on the productivity of formate is investigated as well. Under solar light (solar simulator, AM 1.5 filter) the productivity with TiO₂ is 36.7 mM formate/g cat-hr in the presence of glycerol, which is significantly higher than 2-propanol (2 mmol/hr.gm.catalyst). When illuminated with similar intensity 365 nm light with the photon energy high enough to excite valence band to conduction band electronic transitions in the TiO₂, the productivity of TiO₂ dramatically improves. A remarkably enhanced yield of formate (270 mM formate/g cat-hr) is achieved under solar light using gold- TiO₂ composite in the presence of glycerol as a hole scavenger. In contrast, no effect of gold nanoparticles was observed under 365 light. The improvement in product yield under visible light is attributed to the plasmon resonance induced hot electron transfer from gold nanoparticles to TiO₂. In addition, we studied the Au nanoparticle/ TiO₂-catalyzed photoreduction of resazurin and photooxidation of Rhodamine B in parallel. As expected the addition of gold with TiO₂ improves the photoreduction of resazurin to resorufin under solar light. Surprisingly, gold nanoparticles adversely affected the photo-degradation rate of rhodamine B under both solar light and 365 nm light. This may be because of hydroxyl radical scavenging by gold nanoparticles.





Poster Session

**Tuesday, May 16
11:40am-1:30pm**

Comparison of Reaction of Synthesized and Commercial Manganese Oxide with Bisphenol A

Nabil Shaikh¹, Kateryna Artyushkova¹, Abdul-Mehdi Ali¹,
Huichun Zhang², Jose M. Cerrato¹

¹University of New Mexico, ²Temple University

Water reuse has become an important topic in arid regions such as New Mexico which experience extended dry seasons. However, an emerging class of synthetic organic micropollutants have been increasingly detected in natural waters due to anthropogenic activities. The removal of these contaminants from water is an emerging topic of interest, with good efficacy observed using Manganese Oxides (MnOx) which are naturally abundant redox active metal oxides. However, little is known about the surface interaction during the reaction of MnOx with micro-pollutants. Additionally, most studies utilize pure synthesized MnOx (Syn-MnOx), instead of naturally or commercially available MnOx (Com-MnOx).

This study investigates the reaction of MnOx with micro-pollutants using X-ray Photoelectron Spectroscopy for surface analysis, ICP-Mass Spectroscopy and HPLC for liquid analysis. The surface of Com-MnOx and Syn-MnOx were examined for variations in elemental composition, Mn oxidation state and carbon/oxygen bonding. The solutions were analyzed for dissolved Mn and BPA removal. From Mn3p fitting and Mn3s multiplet splitting, both media showed reduction of Mn on the surface (oxidation state of Mn decreased from 3.8, 3.9 to 3.6, 3.5 for Syn-MnOx and Com-MnOx respectively) and solution samples showed increasing concentration of soluble Mn suggesting reductive dissolution of both media. The BPA removal efficacy of 99.7% for Syn-MnOx and 69.1% for Com-MnOx was observed while the release of dissolved Mn was 14.2 mg/l for Syn-MnOx and 1.1 mg/l for Com-MnOx after 2 days of batch reaction.

Despite these different values, the BPA removal was a function of Mn content of media while the Mn release depended on the surface area of the media. Furthermore, analysis of C1s and O1s XPS spectra indicates towards presence of adsorbed organic reaction products and differences in adsorption behavior of the media. The results have implications for practical application of MnOx in engineered systems for micro-pollutant treatment.



Investigating the Performance of Pd/3D-Graphene Nanocomposites In Anion Exchange Membrane Fuel Cells

Sadia Kabir¹, Alexey Serov¹, Plamen Atanassov¹

¹University of New Mexico

With the recent developments of high performance anion exchange membranes, there has been an increased interest towards implementing AEM fuel cells (AEMFC) for numerous electrocatalytic applications. Previous have demonstrated the improved intrinsic activity, stability and accessibility of Palladium/Graphene-based nanocomposites for ORR in alkaline electrolytes[1-2], although their integration into operating AEMFCs have been quite limited to date. This is mainly due to the challenges associated with (i) synthesizing Pd nanoparticles without surfactants and organic stabilizers (ii) fabricating porous graphitized supports with controlled morphologies that can form triple phase boundaries and (iii) a lack of standardization and optimization for integrating these nanocomposite materials into the membrane electrode assemblies of AEMFCs.

To mitigate the limitations associated with TPB structure and subpar catalytic activities, in this study: macroporous three dimensional Graphene nanosheet (3D-GNS) supports with controlled morphologies and porosities were fabricated by utilizing sacrificial silica templates. The sacrificial templates were then etched to leave a network of porous channels within its matrix, and utilized as supports for Pd nanoparticles. The Pd/3D-Graphene composite materials were also integrated into a catalyst coated membrane, optimized (assembly, activation, electrode fabrication) and analyzed for their performance in H₂O₂ fed AEMFCs operating at 60°C.

Preliminary results showed that conditioning of the membranes was crucial for reducing ohmic losses, whereas porosity of the supports was imperative for facilitating mass transport kinetics. The results in this study further highlights the importance of rationally designing nanomaterials for high-performance energy conversion devices such as fuel cells, and can also be expanded to other energy storage and conversion applications such as electrodes for Li-air batteries and electrolyzers.

[1] S. Kabir, A. Zadick, P. Atanassov, L. Dubau, M. Chatenet, *Electrochemistry Communications*, 2017; 78:33-37.

[2] S. Kabir, A. Serov, K. Artyushkova, P. Atanassov, *Electrochimica Acta*, 2016; 203:144-153



Gelatin Characterization for Tissue Biomimetic for Studying the Mechanisms Blast Induced Traumatic Brain Injuries

Joseph Kerwin¹, Anna Wermer¹, Kelsea Welsh¹

¹New Mexico Institute of Mining and Technology

Blast-induced traumatic brain injury (bTBI) has become a widespread problem for military personnel in recent decades. The mechanisms that cause primary bTBI remain poorly understood, but may be involved in the development of post-traumatic stress disorder. Primary bTBI is characterized when a shock wave causes damage directly to the brain tissue after it propagates through the skull. Whereas, secondary and tertiary bTBI involves damage caused by physical movement from a shock wave. With better understanding of the mechanisms for primary bTBI, researchers could develop better protective equipment for military personnel. To do this, accurate representation of the brains response to bTBI will need to be performed. Thus, brain tissue properties need to be biomimetically represented. Four gelatin-based materials have been characterized through tensile, compression, and shear tests to ensure they accurately mimic brain tissue under stress: bovine bone, bovine skin, 10 and 20% ballistic gelatin. Bovine skin gelatin properties proved to be the most consistent with those presented in literature for brain tissue, with a density of 1.098 g/mL, Young's modulus of 4.614 psi, and fracture strength of 3.28 psi. The average shear storage and loss moduli were found to be 0.5945 psi and 0.05698 psi with a standard deviation of 0.1592 and 0.06375 respectively, at 0.02 atm overpressure and 0.1 s⁻¹. Furthermore, polyester is being studied under similar methods to determine its appropriate use for a skull material. These findings provide a promising direction for research in the mechanisms of bTBI.



Direct Photocatalytic Reduction of Bicarbonate to Formate on Plasmonic Metallic Nanoparticles

Keeniya-Gamalage-Gehan De Silva¹, Hanqing Pan¹,
Michael Heagy¹, Sanchari Chowdhury¹

¹New Mexico Institute of Mining and Technology

A remarkably enhanced yield of formic acid (~270 mM formic acid/g cat-hr) is observed by photoreduction of bicarbonate under solar light using ~15 nm gold nanoparticles in the presence of glycerol as a hole scavenger. Interestingly, the productivity of formic acid using gold nanoparticle catalysts was found to be even higher than conventional TiO₂ nanocatalysts. For both of the photoreduction reactions, 15 nm gold nanoparticles were more efficient than 50 nm Ag nanoparticles. The enhanced efficiency of gold nanoparticle is attributed to their higher light absorption efficiency. In addition, we studied the Au nanoparticle catalyzed photoreduction of resazurin in parallel. Photoreduction of Resazurin to Resorufin in the presence of hydroxylamine as the hole scavenger is a commonly used model reaction to study photocatalytic reduction on nanocatalysts. To understand the mechanism behind enhanced photocatalytic reduction on gold nanoparticles, we studied the reaction under different light wavelengths.



Physical Vapor Deposition of Explosive Materials

Michael Marquez¹, Robert Knepper¹, Alexander Tappan¹

¹Sandia National Laboratories

Physical vapor deposition is an attractive method to produce sub-millimeter explosive samples for studying detonation behavior and microstructure effects. Through the use of shadow masks, we are able to define geometry patterns with sub-millimeter resolution. The deposition of explosive materials can range from 1 - 500 microns in thickness. By varying deposition conditions, we can precisely control microstructure of the deposited films. Metal films can also be deposited in the same vacuum chamber to layer with explosive materials for the purpose of modifying surfaces or confining an explosive layer. This presentation will discuss the challenges related to deposition of explosive materials and provide SEM micrographs of the range of possible microstructures.



Three Dimensional Structural Analysis of Electrodes for Fuel Cells and Electrolyzers Using FIB-SEM

Md Mosaddek Hossen¹, Kateryna Artyushkova¹,
Michael Workman¹, Alexey Serov¹, Plamen Atanassov¹

¹The University of New Mexico

The durability and performance of platinum group metal-free (PGM-free) catalyst depend on the chemical composition and morphological properties of the catalyst such as porosity, roughness, and texture. The pore structure is critical to the transport of oxygen to active sites and removal of water. Anodes based on PGM-free electrocatalysts for alkaline exchange membrane fuel cells (AEMFC) were studied by XPS, FIB-SEM and electrochemical testing. A three-dimensional reconstruction of electrodes is effectively investigated using the focused ion beam-secondary electron microscope (FIB/SEM), providing critical information on three-dimensional morphology. Useful information from the 2D and 3D representation of electrodes was extracted by calculating key structural parameters such as overall roughness, porosity, tortuosity, connectivity, average solid phase size and average pore size. Post-mortem analysis of electrodes for electrolyzers has been performed based on the imaging of 2D cross section created by FIB. Different parameters i.e. roughness, pore sizes, skewness, porosity, etc. have been compared between the sample before and after operation in the electrolyzer. The initial composition of the electrode structures affected the changes in morphology of the samples that occurs during testing.



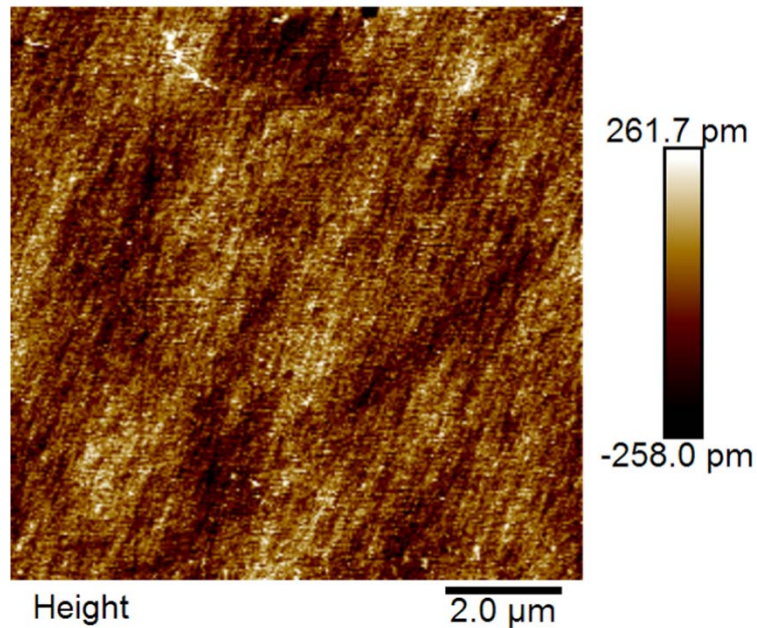
Precision Backside Si Thinning to Land on Thin Films

Morgan O'Mahony¹, Adam Jones¹, John Mudrick¹, Elijah Madison¹,
Jonatan Sierra Suarez¹

¹Sandia National Laboratories

Problem Statement:

- Need to remove handle Si (640mm thick) to land on dielectric (ARC); loss tolerance <5nm
- Final thinning uniformity must be <1mm
- Sensitive to scratches transferred to ARC layer and embedment of slurry particles in the substrate
- Process requirements strain tool capabilities
- Excellent tool qualification and repeatability required



Surface roughness data from AFM of a part polished with Best Known Method discovered by the experiment.

C-H Bond Activation on Single-Site Active Porous Sheet: Catalytic Conversion of Methane to Methanol

Thalia Quinn¹, Joseph Kerwin¹, Pabitra Choudhury¹,
Sierra Headrick¹, Sean Mussel¹

¹New Mexico Institute of Mining and Technology

Catalysts are needed in applications regarding the world's fuel and chemical production. To assist these processes, catalysts are used to simplify the chemical reaction by lowering the energy required for reactions to complete. The goal of our project is to identify and characterize specific catalysts through computational research and more specifically the conversion from natural gas to liquid feedstock. Previous work shows that the hydrogen affinity of a structure, the energy needed to move electrons in a reaction, can be directly linked to the reactivity of a catalyst for conversions involving hydrocarbons. By recognizing the correlation between hydrogen affinity, C-H bond activation, and transition state activation energy, new optimal catalysts based on a single-site active porous surface can be identified for the target conversion. Also, this work will support the idea of not only decreasing the computational costs for future simulation, but also reducing the future experimental efforts by providing the necessary inputs to experiments.



Target Conversion: Methane to Methanol



Theoretical Study of a High Performance Thermoelectric Material: Stanene

Charles Griego¹, Pabitra Choudhury¹, Joshua Livingston¹

¹New Mexico Institute of Mining and Technology

Improving the efficiency of power generation while reducing the amount of energy waste is a crucial step towards sustainability. High performance thermoelectric materials with the capability of converting waste heat to electricity are a potential solution to step away from an energy crisis. In recent years, the research towards finding new candidates for such applications has gone to great lengths. Specifically, the reduction of low-dimensional materials to the nanoscale has produced fascinating results regarding the improvement of thermoelectric performance. In this study, we investigate the enhancement of the thermoelectric figure of merit for stanene between nanoribbon form and the bulk using first-principles calculations. The thermopower properties were calculated using combined first-principles calculations and Boltzmann transport theory within the relaxation time approximation calculated from deformation potential theory. We find that bulk stanene exhibits a thermoelectric figure of merit that is near half of unity at the optimum doping level. We propose that the thermoelectric capabilities of stanene are enhanced further for armchair and zigzag edged nanoribbon structures.



Optimizing a Plasma Process for Creating Black Silicon

Michael Salcido¹, Todd Bauer¹

¹Sandia National Laboratories

Black silicon is the result of surface modification of single crystal silicon where the surface modification causes scattering of incident visible light. The micro- and nano-scale physical structures that result in scattering also create higher surface area than a planar single crystal silicon surface, which has application in energy conversion in photovoltaics as well as chemical and physical processes that require high surface area to volume ratio. In this poster we present a plasma etch process for creating black silicon on 150 mm single crystal silicon wafers. To modulate surface modification, we systematically varied RD power and gas mixtures including SF₆, O₂, C₄F₈, and CO in a commercial capacitively coupled plasma etch chamber. We also investigated the effect of chamber seasoning on surface modification. We quantified surface modification using an ultraviolet laser confocal microscope to measure the topography imparted to silicon wafers. Small amounts of C₄F₈ added to a much larger flow of SF₆ and O₂ maximizes surface modification as determined by the RMS roughness of the resulting silicon surface. RMS roughness was also measured to be dependent on chamber condition which led to the development of a chamber seasoning sequence.

Sandia National Laboratories is a multimission laboratory managed and operated by National Technology and Engineering Solutions of Sandia, LLC., a wholly owned subsidiary of Honeywell International, Inc., for the U.S. Department of Energy's National Nuclear Security Administration under contract DE-NA-0003525.



Creating Facets in Photoresist Using Plasma Etch Processing

Erin Sovey¹, Todd Bauer¹

¹Sandia National Laboratories

We present a method for creating non-vertical facets at the edge of patterned photoresist features. The presence of facets in a photoresist layer can create sidewall tapering in subsequent plasma etches as the resist facet translates into the underlying film. Sidewall tapering can be useful for various applications, including maintaining continuity of diffusion barrier films or conductive films deposited over topography. We explored our process parameters in a commercial inductively coupled plasma reactor with systematic variations in gas flow (Ar, CF₄ and O₂ gases) and RF bias power, and achieved tunable sidewall angles ranging from vertical to 65 degrees from horizontal.

Sandia National Laboratories is a multimission laboratory managed and operated by National Technology and Engineering Solutions of Sandia, LLC., a wholly owned subsidiary of Honeywell International, Inc., for the U.S. Department of Energy's National Nuclear Security Administration under contract DE-NA-0003525.



Study of Effects of Organic Matter and Uranium Binding (Release) from Abandoned Mine Lands in the Southwestern United States

Carmen A. Velasco¹, Sumant Avasarala¹, Abdul-Mehdi Ali¹,
Kateryna Artyushkova¹, José M. Cerrato¹

¹University of New Mexico

We applied spectroscopy, microscopy, and water chemistry techniques to investigate the effects of organic matter on uranium (U) binding from abandoned U mine waste from the Jackpile Mine in Laguna Pueblo, New Mexico. Preliminary studies using fixed angle X-ray fluorescence (XRF) analysis show 3.14% carbon (C). Results from microprobe mapping suggest that uranium particles are surrounded by carbon inclusions. We hypothesize that the presence of carbon in the mine waste influences the uranium binding and therefore its release to the environment. Loss on ignition (LOI) analyses showed that 12.98±0.25% mass was lost for particles size <63 µm and 46.17±3.04% mass was lost for particles size between 2-4.75mm. The change on mass after the LOI might be due to the loss of organic content of the samples. Analyses with X-ray photoelectron spectroscopy (XPS) show changes on the carbon binding after the LOI experiments and the oxidation of U (IV) to U(VI). The mean concentration of acid extractable uranium for mine waste particles of <63 µm was 0.54±0.1% U before LOI and 0.64±0.01% U after LOI. The mean concentration of acid extractable uranium for mine waste particles of 2-4.75mm was 0.79±0.25% U before LOI and 5.4±0.5%U after LOI. This study identified the relevance of considering the binding of U and C in mine wastes to better understand U mobilization in the environment.





Session 3

**Tuesday, May 16
1:30pm-3:00pm**

Moderator: Erica Douglas

1:30 pm

Graphene-Based Charge-Coupled Devices for Sensitive Optical Detection

Stephen Howell¹, Thomas Beechem¹, Isaac Ruiz¹, Paul Davids¹,
Richard Harrison¹, Sean Smith¹, Michael Goldflam¹, Nicholas Martinez¹,
Jeffery Martin¹

¹Sandia National Laboratories

We will present our research on the development of sensitive optical detectors based on a graphene charge - coupled device architecture. Graphene is emerging as an interesting material for photosensing applications spanning the electromagnetic spectrum (ultraviolet to terahertz). In practical applications, achieving high sensitivities remains elusive due to the difficulty of coupling light into an atomically thin layer. To circumvent this issue, we have developed a photodetector concept based on a graphene field effect transistor (GFET) that is capacitively coupled using a thin dielectric layer to a thick semiconducting absorber. Unlike other graphene-based detector concepts, absorption of photons takes place in the semiconducting substrate and not the ultra-thin graphene layer. The GFET acts as a sensitive local charge detector, sensing photo-induced charge that collects in the potential well that forms at absorber/dielectric interface during deep depletion. As photo-charge collects within the potential well, the GFET's conductivity is altered due to the presence of capacitively-coupled substrate charge that forms within the graphene channel. The behavior of this hybrid device is analogous to a self-sensing metal/oxide/semiconductor (MOS) capacitor, which is the fundamental building block of modern CCD imaging technology.

We have successfully fabricated device arrays using commercial CVD graphene transferred atop HfO₂ deposited on a low-doped n-type silicon. Responsivities as high as 2500 A/W (25,000 S/W), for visible wavelengths, have been observed using moderate integration times. Consistent behavior for multiple devices fabricated on different chips was also observed, with signal-to-noise ratios comparable to commercial CCD technology. Although similar devices have been fabricated previously, an improved understanding of the working principles for this device, along with a semi-analytical model, will also be presented.



Sandia National Laboratories is a multi-program laboratory managed and operated by Sandia Corporation, a wholly owned subsidiary of Lockheed Martin Corporation, for the U.S. Department of Energy's National Nuclear Security Administration under contract DE-AC04-94AL85000. This work is supported by Sandia's LDRD Program.

1:50 pm

Temperature Dependence of the Dielectric Function of Bulk Ge

Carola Emminger¹, Nuwanjula Samarasingha¹, Farzin Abadizaman¹,
Nalin Fernando¹, Stefan Zollner¹

¹New Mexico State University

Many of the Ge applications depend on the dielectric function (ϵ), which is directly related to the electronic band structure. Here we investigate the effect of temperature on the optical properties and interband critical points (CPs), primarily the E_0 and $E_0+\Delta_0$ critical points of bulk Ge in the temperature range from 10 to 738 K using spectroscopic ellipsometry at 70° angle of incidence from 0.5 eV to 6.2 eV with 10 meV steps. The low temperature environment was created in a UHV cryostat with liquid helium and nitrogen as cryogens. To reduce the thickness of the native GeO_2 layer, the Ge sample was cleaned using ultra-pure water, isopropanol, an ultrasonic bath and ozone cleaning. It was possible to reduce the oxide thickness to about 11 Å at room temperature.

The authors used a two-phase model (GeO_2 layer/Ge substrate) and a parametric oscillator model with a set of adjustable parameters to extract the real and imaginary parts of the complex dielectric function of bulk Ge for the whole temperature range. To investigate the temperature dependence of the CP parameters (threshold energy, broadening and phase angle) further, we also compared the second derivative $d^2\epsilon/d^2\omega$ of the dielectric function with analytical line shapes.

The temperature has a significant influence on both the real and imaginary parts of the complex dielectric function of bulk Ge. This temperature dependent ϵ can be explained by a Bose-Einstein occupation factor. Due to the electron-phonon interaction, we find a temperature dependent red shift (shift to lower energies) of the E_0 and $E_0+\Delta_0$ critical point energies. The temperature independent spin orbit splitting Δ_0 is found to be 286 meV. A similar effect has been seen in the E_1 , $E_1+\Delta_1$, E_0' , and E_2 CP energies. These CPs are broadened and shifted to lower energies with increasing temperature.

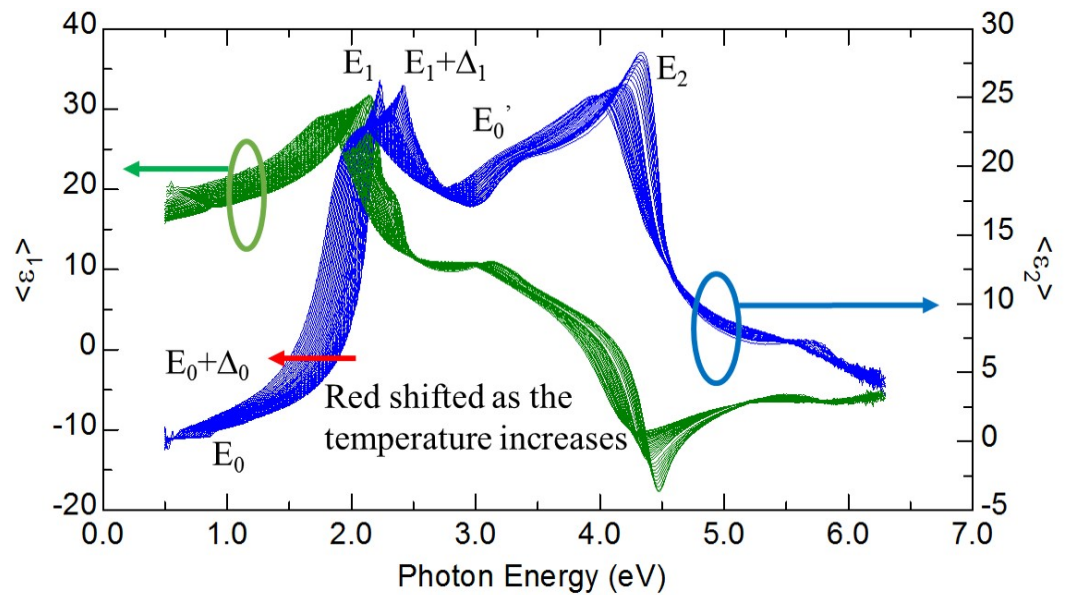


1:50 pm
Continued

Temperature Dependence of the Dielectric Function of Bulk Ge

Carola Emminger¹, Nuwanjula Samarasingha¹, Farzin Abadizaman¹,
Nalin Fernando¹, Stefan Zollner¹

¹New Mexico State University



Real and imaginary parts of the pseudo-dielectric function of bulk Ge as a function of photon energy in the temperature range from 10 to 738 K.



2:10 pm

Near-Infrared to Vacuum Ultraviolet (VUV) Dielectric Properties of LaAlO_3

Jacqueline Cooke¹, Tom Tiwald², Nuwanjula Samarasingha¹,
Nalin Fernando¹, Stefan Zollner¹

¹New Mexico State University, ²J.A. Woollam Co.

Lanthanum Aluminate (LaAlO_3) is a ceramic oxide with a perovskite structure of ABO_3 . It is used as a substrate material for oxide epitaxy and as an insulator. Quite a bit of research has been done for lanthanum aluminate when it is epitaxially grown on strontium titanate (SrTiO_3) as it causes some unique properties to occur at the interface. And yet not much is known about lanthanum aluminate. Here we use spectroscopic ellipsometry to determine the dielectric function and absorption coefficient of lanthanum aluminate. A single-side polished wafer was used for spectroscopic ellipsometry and a two-side polished wafer with 0.2 mm thickness was used for transmission measurements. A J.A. Woollam variable angle of incidence ellipsometer with a computer-controlled Berek waveplate compensator was used for transmission and spectroscopic ellipsometry measurements. To measure at higher energies, a J.A. Woollam VUV VASE ellipsometer was used. The spectroscopic data was taken between 0.5 and 9 eV with 0.02 eV steps between 60° and 75° angle of incidence with 5° steps at room temperature. The transmission measurements were taken between 0.8 and 6.5 eV with 0.02 eV steps at normal incidence and room temperature. The ellipsometric angles were then modeled by describing the dielectric function using a sum of Kramers-Kronig consistent oscillators. The transmission and ellipsometry data is used to calculate the absorption coefficients between 0.8 and 6.5 eV as well as the onset of absorption.



2:30 pm

Spectroscopic Surface Study of Manganese Oxides Reaction with Organic Micropollutants

Nabil Shaikh¹, Kateryna Artyushkova¹, Abdul-Mehdi Ali¹, Huichun Zhang²,
Jose M. Cerrato¹

¹University of New Mexico, ²Temple University

Water reuse has become an important topic in arid and semi-arid regions such as New Mexico which experience extended dry seasons. However, an emerging class of synthetic organic micropollutants have been increasingly detected in natural waters due to anthropogenic activities. These contaminants, even in trace concentrations, have been known to negatively affect the aquatic ecosystem and be noxious to humans if chronically exposed. Manganese Oxides (MnOx) are naturally abundant oxides with good reactivity with most organic micropollutants, however little is known about the surface interaction during the reaction.

The investigation of MnOx surface after reaction with organic micropollutants such as Aniline, Phenol and Triclosan was carried out using X-ray Photoelectron Spectroscopy and Raman Spectroscopy. Additionally, solution chemistry was performed using ICP-Mass spectrometry and High Performance Liquid Chromatography to help understand the interfacial chemistry. The surface of unreacted and reacted MnOx were examined for variations in Mn oxidation state and carbon/oxygen bonding. The solutions were analyzed for soluble Mn. Reaction of phenol with MnOx resulted in increase in C-OH and C-O-O-C bonds, indicating the presence of phenol and its polymeric by-products. Detection of chlorine after reaction with triclosan, suggests that triclosan and its by-products are associated to MnOx surface. The increase in aromatic and aliphatic carbon bonds after reaction with aniline suggests that aniline and its byproducts are also associated to MnOx surface. An increase of Mn(III) on surface and dissolution of Mn into solution was detected for reacted MnOx, indicating reduction of MnOx. Different changes in the MnOx surface was observed among the organic compounds, indicative of differing mechanism or pathways of surface reactions for different organic groups. Removal of organic compounds varied (triclosan, phenol, aniline) due to various factors such as passivation of surface sites, and influence of substituent.

Reference: Shaikh et. al, Environ. Sci. Technol. 50, 10978-10987 (2016)





Session 4

**Tuesday, May 16
3:00pm-5:00pm**

Moderator: Linnea Ista

3:00 pm

Design of a Time-of-Flight Secondary Ion Mass Spectrometer for Hands-on Undergraduate Instruction

Michael Lee¹, Ben A. Hardesty¹, Riley T. Ducey¹,
Sharna E. Beahm¹, Isaiah F. Cons¹

¹Northern Arizona University

Time-of-Flight Secondary Ion Mass Spectrometry (TOF-SIMS) is one of the most advanced mass spectrometry techniques. High-end TOF-SIMS is capable of mass resolution ($m/\Delta m$) $>10,000$, mass accuracy >1 ppm with potentially unlimited mass range, and lateral spatial resolution better than 100 nm. Unfortunately, cutting-edge instruments such as TOF-SIMS are far beyond the resources of undergraduate programs. Students are often not even exposed to advanced instrumentation, or to the inner-workings of instrumentation unless they pursue graduate work. Here we share our experience and progress on building a basic TOF-SIMS instrument with undergraduate students. The instrument has reduced specifications, but nears the price range that is possible for undergraduate degree programs. Interdisciplinary collaboration between the chemistry and engineering departments is critical for integrating commercially available pieces into a working system. Engineering undergraduate students are working with chemistry undergraduate researchers to properly design and build the system. The system is intended for an undergraduate instruction in analytical chemistry at our university and will form the basis for future collaborative projects with the engineering department.



3:00 pm
Continued

Design of a Time-of-Flight Secondary Ion Mass Spectrometer for Hands-on Undergraduate Instruction

Michael Lee¹, Ben A. Hardesty¹, Riley T. Ducey¹,
Sharna E. Beahm¹, Isaiah F. Cons¹

¹Northern Arizona University

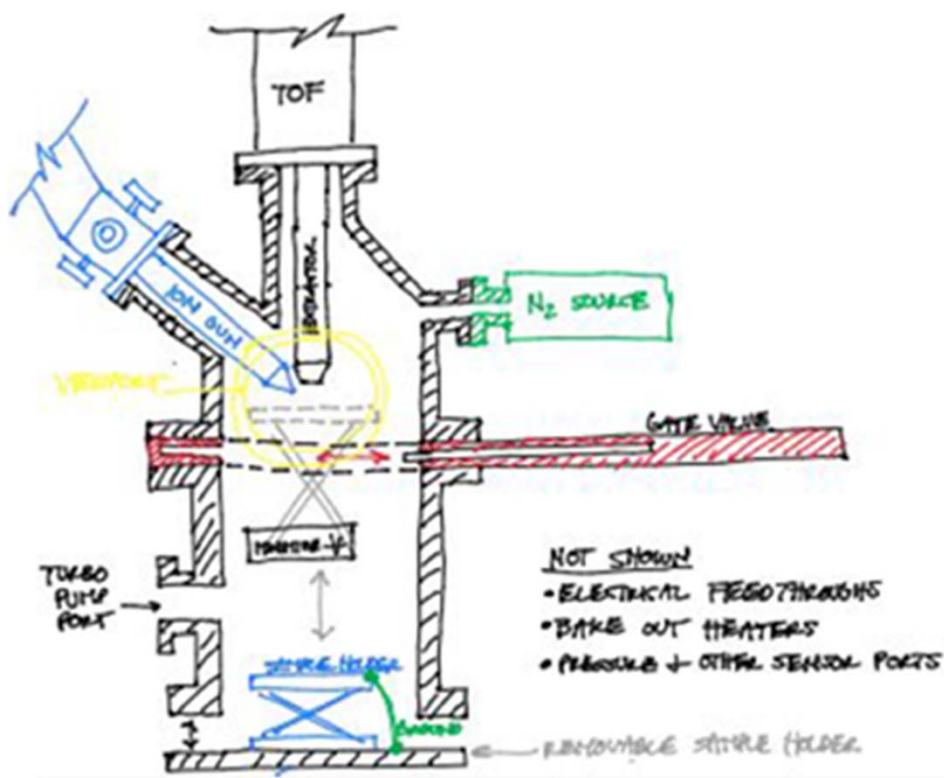


Figure 1. Example of design ideas generated by undergraduate students for a basic TOF-SIMS system

3:20 pm

Temperature Dependent Mueller Matrix Measurements of Magnetised Ni near the Curie Temperature

Farzin Abadizaman¹, Stefan Zollner¹

¹New Mexico State University

The temperature dependence of the optical constants of the magnetized bulk Ni demonstrates an anomaly near the Curie temperature. We investigate this anomaly by taking a measurement of the temperature dependent Mueller Matrix (MM). Using spectroscopic ellipsometry at an energy 1.96 eV, the MM measurement was taken from 350 K to 500 K with 10 K steps, and from 500 K to 670 K with 1 K steps, and from 670 K to 730 K with 10 K steps.

In order to distinguish the anisotropic properties of the magnetized Ni from the windows effects, three samples (Ge, Ni, and SiO₂ on Si) were measured inside the cryostat in the energy range from 1 eV to 5 eV with 0.1 eV steps. The results show that the anisotropic elements of the MM behave in the same fashion for all samples, except for element M_{24} , which depends on the sample.

The MM data of magnetized Ni indicate very small changes in the anisotropic portion of the MM compared to the windows effect. The authors believe that these changes are due to the magneto-optical Kerr effect. However, since a rotating-analyzer ellipsometer was used, the last row of the MM is absent and a complete MM measurement needs to be performed to find the magneto-optical Kerr effect in the other anisotropic elements too.

However, very large decreases in the isotropic MM elements were found near the Curie temperature. This means, the changes in optical constants near T_c are due to the on-diagonal Drude part of the dielectric tensor, which can be explained by s- to d-band electron-phonon scattering above and below T_c . These changes are absent when decreasing the temperature and for unmagnetized Ni.



3:40 pm

Microsphere-Based Disordered Coatings for Effective Radiative Cooling

Sarun Atiganyanun¹, John Plumley¹, Kevin Hsu¹,
Jacob Cytrynbaum², Thomas Peng³, Sang M. Han¹, Sang Eon Ha¹

¹University of New Mexico, ²Williams College,
³Air Force Research Laboratory

Being able to cool the buildings below the ambient temperature under the sun in the middle of a summer without having to use air conditioning would result in tremendous energy savings. As a step towards this goal, we have investigated a facile application of coatings made of silica microspheres in disordered structures, using evaporation as well as spray-coating. For the evaporation coating, silica microspheres are dispersed in water, and the colloidal stability is disrupted by dissolving ionic salt into the solution. The colloidal solution is confined onto a substrate and is allowed to evaporate. For the spray-coating, much like commercial painting, the aqueous colloidal solution is forced through a spray nozzle and deposited onto a substrate. Scanning electron microscopy images and autocorrelation analyses show that the resulting structures are disordered without short- or long-range order. Optical measurements also indicate that the coatings produced under optimal conditions have a short transport photon mean free path of approximately 4-8 μm in the solar spectral region. These coatings exhibit high emissivity above 95% in the atmospheric transparency window. These results suggest strong photon scattering properties in the visible region, while providing a strong thermal emission. Such films would enable effective radiative cooling. To estimate the theoretical limit, a computational model is first used to calculate the cooling power of the coatings under direct sunlight. The model predicts that the disordered coating with 200 μm thickness has a cooling power of $\sim 250 \text{ W/m}^2$ at 27°C and could reduce the temperature of the sample under the direct sunlight by approximately 37°C below the ambient temperature. Our experimental measurements under direct sunlight show that our coatings perform better than commercial sunlight and heat reflective paints. We will further discuss how coatings of disordered, random, inverse structures can enhance the durability of our coating in a paint format, while maintaining radiative cooling properties.



4:00 pm

Fe-N-C PGM-free ORR Catalysts Derived by C-N-C Backbone Polymerization-Pyrolysis Method

Yechuan Chen¹, Rohan Gokhale¹, Alexey Serov¹,
Kateryna Artyushkova¹, Plamen Atanassov¹

¹University of New Mexico

Recently metal-nitrogen-carbon (M-N-C) type catalysts for oxygen reduction reaction in fuel cell cathode have gained more and more interests as promising candidates to replace platinum group metal (PGM) based conventional electrocatalysts. Among numerous methods utilized to synthesize M-N-C catalysts, sacrificial support method (SSM) that was developed by the group in University of New Mexico uses silica template to prepare high performance iron-nitrogen-carbon (Fe-N-C) composites for fuel cell cathode. Based on this method, a C-N-C backbone polymerization pyrolysis from aminopyridine and benzimidazole is adopted to synthesize nanoporous ORR catalysts. Different from previously investigated nitrogen contained polymers such as polypyridine and polyaniline, this novel polymerization pyrolysis method is the first time to utilize C-N-C backbone poly-pyridine and poly-benzimidazole for synthesis. With the introduction of persulfate salts into well dispersed mixture of precursors and silica in water, amino groups could lose hydrogen atoms to form new nitrogen-carbon bonding with other monomers. The preformed nitrogen-carbon network before pyrolysis leads to final catalysts with high performance in both acid and base environment. In addition to half-wave potential approaching 0.87 V vs RHE in base and 0.75 V in acid (the candidate prepared from 2-amino-6-pyridine), these materials also have low peroxide percentage (lower than 2% in diffusion section), achieving the target of Department of Energy.

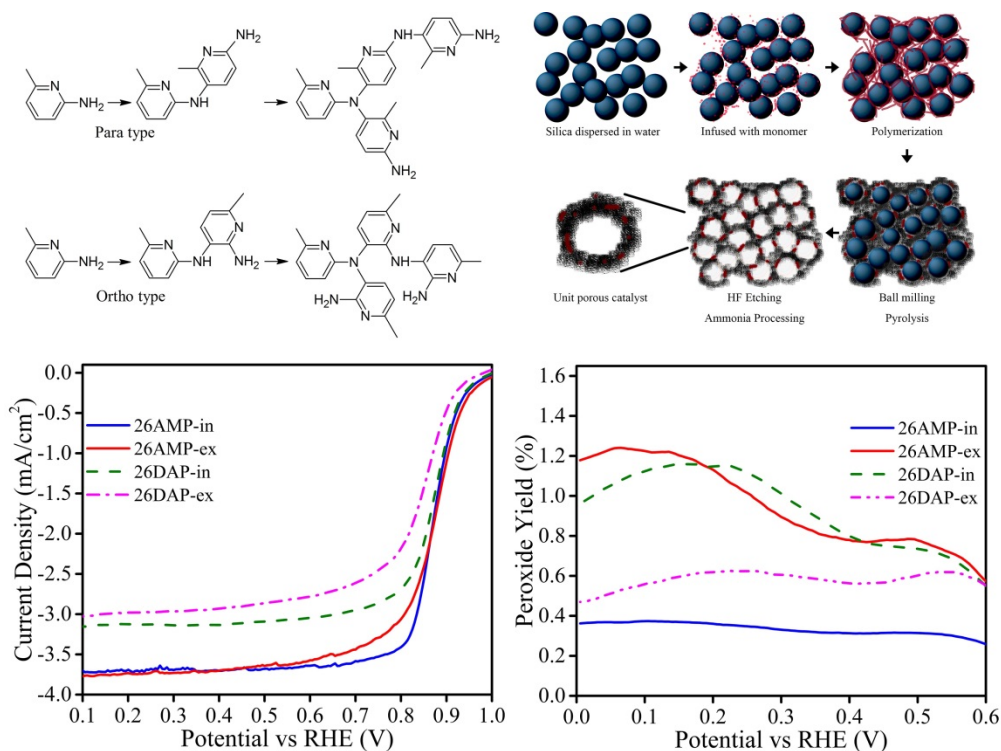


4:00 pm
Continued

Fe-N-C PGM-free ORR Catalysts Derived by C-N-C Backbone Polymerization-Pyrolysis Method

Yechuan Chen¹, Rohan Gokhale¹, Alexey Serov¹,
Kateryna Artyushkova¹, Plamen Atanassov¹

¹University of New Mexico



Top: the polymerization and synthesis diagrams

Bottom: the cyclic voltammety plots of catalyst performance and peroxide percentage in 1M KOH